Asymmetry of the GroEL-GroES Complex under Physiological Conditions as Revealed by Small-Angle X-Ray Scattering

Tomonao Inobe,* Kazunobu Takahashi,*† Kosuke Maki,*† Sawako Enoki,* Kiyoto Kamagata,* Akio Kadooka,* Munehito Arai,* and Kunihiro Kuwajima*†‡

*Department of Physics, School of Science, University of Tokyo and CREST, Japan Science and Technology Agency, Tokyo 113-0033, Japan; †Okazaki Institute for Integrative Bioscience, National Institutes of Natural Sciences, Okazaki 444-8787, Japan; and ‡Department of Functional Molecular Science, School of Physical Sciences, Graduate University for Advanced Studies SOKENDAI, Okazaki 444-8787, Japan

ABSTRACT Despite the well-known functional importance of GroEL-GroES complex formation during the chaperonin cycle, the stoichiometry of the complex has not been clarified. The complex can occur either as an asymmetric 1:1 GroEL-GroES complex or as a symmetric 1:2 GroEL-GroES complex, although it remains uncertain which type is predominant under physiological conditions. To resolve this question, we studied the structure of the GroEL-GroES complex under physiological conditions by small-angle x-ray scattering, which is a powerful technique to directly observe the structure of the protein complex in solution. We evaluated molecular structural parameters, the radius of gyration and the maximum dimension of the complex, from the x-ray scattering patterns under various nucleotide conditions (3 mM ADP, 3 mM ATPγS, and 3 mM ATP in 10 mM $MgCl_2$ and 100 mM KCl) at three different temperatures (10°C, 25°C, and 37°C). We then compared the experimentally observed scattering patterns with those calculated from the known x-ray crystallographic structures of the GroEL-GroES complex. The results clearly demonstrated that the asymmetric complex must be the major species stably present in solution under physiological conditions. On the other hand, in the presence of ATP (3 mM) and beryllium fluoride (10 mM NaF and 300 μM $BeCl_2$), we observed the formation of a stable symmetric complex, suggesting the existence of a transiently formed symmetric complex during the chaperonin cycle.

INTRODUCTION

The chaperonins are ubiquitously found in bacteria, archaea, and eukarya—a class of molecular chaperones that promote protein folding in vivo (1,2). The best characterized of these is the *Escherichia coli* chaperonin, GroEL, and its partner GroES (1–5). GroEL is a tetradecameric protein of 14 identical 57 kDa subunits arranged in two heptameric rings stacked back-to-back with a central cavity (6,7). GroES contains seven identical 10 kDa subunits assembled as a heptamer ring and acts as a lid of the central cavity when GroEL forms a complex with GroES (7,8). Under physiological conditions, GroEL and GroES form this complex, and the complex formation seems to be essential for the biological functions. A substrate protein in the chaperonin-assisted folding is known to be encapsulated within the central cavity of the GroEL-GroES complex and to fold in this location (7,9).

Despite the well-known functional importance of GroEL-GroES complex formation, the stoichiometry of the complex has not yet been fully established. The complex may occur in two different forms: i), one GroES binds to one side of the GroEL oligomer with a 1:1 (GroEL/GroES) stoichiometry to form an asymmetric (bullet-type) complex (10–14), and ii), one GroES binds to both sides of the GroEL oligomer with a stoichiometry of 1:2 (GroEL/GroES) to form a symmetric (football-type) complex (15–21). Previous structural studies performed by different groups and employing primarily electron microscopy have reported conflicting results. That is, some of the studies reported that the asymmetric complex was the major species formed under physiological conditions (10–14) and others that the symmetric complex was the main complex formed (16–21), despite the fact that the conditions and solutions used to prepare the complexes were similar. As a result, several research groups have proposed a model in which the symmetric complex is significantly accumulated during the reaction cycle and acts as an important intermediate in the chaperonin function (19–25), whereas other groups have proposed a model in which only the asymmetric complex appears during the reaction cycle (26–30). Although the latter model with the asymmetric complex prevails and seems to be widely accepted, the conflict between the two models has not yet been fully resolved. It is certainly critical in understanding the molecular mechanisms of the chaperonin function to resolve the question about the stoichiometry

Submitted June 9, 2007, and accepted for publication October 10, 2007.

Address reprint request to Kunihiro Kuwajima, Tel.: 81-564-59-5230; Fax: 81-564-59-5234; E-mail: kuwajima@ims.ac.jp.

Tomonao Inobe's present address is Dept. of Biochemistry, Molecular Biology and Cell Biology, Northwestern University, Evanston, Illinois 60208.

Kosuke Maki's present address is Dept. of Physics, Graduate School of Science, Nagoya University, Nagoya 464-8602, Japan.

Sawako Enoki's present address is The Institute of Scientific and Industrial Research, Osaka University, Osaka 567-0047, Japan.

Kiyoto Kamagata's present address is Institute for Protein Research, Osaka University, Osaka 565-0871, Japan.

Munehito Arai's present address is Institute for Biological Resources and Functions, National Institute of Advanced Industrial Science and Technology (AIST), Ibaraki 305-8566, Japan.

Editor: Jill Trewhella.

0006-3495/08/02/1392/11 $2.00

doi: 10.1529/biophysj.107.114710

of the GroEL-GroES complex, and hence further clarification of the stoichiometry by another experimental technique will be useful.

Thus, in this study we employed small-angle x-ray scattering (SAXS) techniques to resolve the above question about the stoichiometry of the GroEL-GroES complex. The SAXS pattern directly reflects the structure of the protein complex in solution, and hence it has an advantage over the techniques previously used for investigating the structure of the GroEL-GroES complex (31–34). To investigate the structure of the GroEL-GroES complex in solution under physiological conditions, we measured the SAXS patterns of the complex under various nucleotide conditions in the presence of ADP, ATPγS, or ATP (3 mM) in 50 mM Tris-HCl, 10 mM $MgCl_2$, and 100 mM KCl at pH 7.5 at three different temperatures, 10°C, 25°C, and 37°C. We measured the SAXS patterns both in the absence and in the presence of a denatured substrate protein (disulfide-reduced α-lactalbumin) (35–37). We observed only the asymmetric complex under all the above conditions, clearly demonstrating that the asymmetric (bullet-type) complex must be the major species stably present in solution under physiological conditions. Our results thus show that the symmetric (football-type) complex does not accumulate significantly during the native chaperonin cycle. However, in the presence of ATP and beryllium fluoride (BeF_x), which may form an analog (ADP·BeF_x) of a transient intermediate of the ATP hydrolysis by GroEL (38–43), we observed the formation of the symmetric 1:2 GroEL-GroES complex, suggesting the existence of a transiently formed symmetric complex during the chaperonin cycle.

MATERIALS AND METHODS

Materials

GroEL and GroES were overexpressed in *E. coli* and purified as described previously (44–46). The overexpression of GroES was also carried out using an expression plasmid, pETESwild, which was a gift of Professor Kawata of Tottori University; GroES was purified using the procedure reported by his group (47). The concentrations of GroEL and GroES were measured by absorption at 280 nm using extinction coefficients, $E^{0.1\%}_{1cm} = 0.21$ for GroEL and $E^{0.1\%}_{1cm} = 0.143$ for GroES (44), which correspond to the molar extinction coefficients of 1.68×10^5 $M^{-1}cm^{-1}$ and 1.04×10^4 $M^{-1}cm^{-1}$, respectively. The molar concentrations of GroEL and GroES shown in this work are those for the GroEL tetradecamer and the GroES heptamer.

Bovine α-lactalbumin was purified from crudely purified powder (Sigma, St. Louis, MO) by ion-exchange chromatography on a diethylaminoethyl-Sepharose fast-flow column with a salt gradient of NaCl from 0 M to 0.3 M. Its concentration was determined spectrophotometrically using an extinction coefficient of $E^{0.1\%}_{1cm} = 2.01$ (48), which corresponds to the molar extinction coefficient of 2.85×10^4 $M^{-1}cm^{-1}$. Apo-α-lactalbumin was prepared by acid denaturation of the protein followed by gel filtration on a Sephadex G-25 column (36). The disulfide-reduced form of α-lactalbumin was prepared by reduction of the disulfide bonds of apo-α-lactalbumin (2 mg/ml) for more than 20 min by 1 mM dithiothreitol (DTT) in 50 mM Tris-HCl, 10 mM $MgCl_2$, and 100 mM KCl at pH 7.65 (36).

The nucleotides ATP, ADP, and ATPγS were purchased from Sigma. ADP and ATPγS were purified by anion-exchange chromatography before use as described (45). BeF_x was prepared as described previously (41). All other chemicals were of guaranteed reagent grade.

Standard buffer

The standard reaction buffer used in all of the experiments described here, except where stated otherwise, was 50 mM Tris-HCl, 10 mM $MgCl_2$, and 100 mM KCl at pH 7.5.

SAXS measurements

The SAXS experiments were performed at beam line 15A of the Photon Factory at the High Energy Accelerator Research Organization, Tsukuba, Japan. The experimental details and the analysis of the scattering data were essentially the same as described previously (48). The scattering patterns were recorded by a charge-coupled device (CCD)-based x-ray detector, which consisted of a beryllium-windowed x-ray image intensifier (Hamamatsu V5445P-MOD; Hamamatsu, Japan), an optical lens, a CCD image sensor, and a data acquisition system (Hamamatsu C7300), as described previously (49,50).

The scattering patterns of the proteins are represented by the scattering intensity I as a function of the momentum transfer Q, which is given by $Q = 4\pi\sin\theta/\lambda$ (λ, wavelength; 2θ, scattering angle). The λ of the x-ray beam was 1.5 Å. The minimum value of Q, Q_{min}, which may depend on the beam stopper size and camera length, was on the order of 0.013 $Å^{-1}$ in our x-ray scattering system.

The pair distance distribution function, $P(r)$, was calculated from the scattering pattern in a Q range of 0.013–0.165 $Å^{-1}$ by the method of Svergun et al. (51) using the GNOM software package, which is based on the regularization of the inversion of the integral equation relating $I(Q)$ to the $P(r)$. The radius of gyration, R_g, and maximum dimension, D_{max}, were thus obtained from the $P(r)$, which is related to R_g by the equation

$$R_g^2 = \frac{\int_0^{D_{max}} r^2 P(r)\mathrm{d}r}{2\int_0^{D_{max}} P(r)\mathrm{d}r}. \quad (1)$$

The R_g and the forward intensity $I(0)$ were also calculated from the Guinier approximation using the innermost portion ($0.013 < Q < 1.4/R_g$) of the scattering patterns by the equation

$$I(Q) = I(0)\exp(-R_g^2Q^2/3). \quad (2)$$

From Eq. 2, the slope and the intercept of the semilogarithmic plot (the Guinier plot) of ln $I(Q)$ versus Q^2 gave the R_g and $I(0)$, respectively. Although the R_g values from the $P(r)$ and the Guinier plot were in general agreement with each other, the relation of R_g to $P(r)$ (Eq. 1), making use of the whole scattering curve, is much less sensitive to factors such as the presence of residual interparticle interactions than is the Guinier approximation (33). The R_g values obtained from the $P(r)$ analysis are thus expected to be more reliable than those from the Guinier approximation.

The SAXS patterns, the $P(r)$ profiles, and the Guinier plots shown in this work are those after extrapolation to zero protein concentration. We measured SAXS patterns at several different protein concentrations and calculated $I(Q)/c$, where c denotes the protein concentration. The SAXS pattern at zero protein concentration was obtained by extrapolation of $I(Q)/c$ to zero protein concentration. The $P(r)$ profiles and the Guinier plots were calculated from the SAXS pattern at zero protein concentration, and the scattering parameter values obtained from the $P(r)$ analysis and the Guinier approximation were, thus, those values at zero protein concentration.

The scattering parameters (R_g and D_{max} from the $P(r)$, and R_g and $I(0)/c$ from the Guinier plot) at zero protein concentration were also obtained by extrapolating these parameter values themselves, which were calculated from the $P(r)$ profiles and the Guinier plots at different protein concentrations, to zero protein concentration. The parameter values at zero protein

concentration thus obtained were coincident with those obtained from the SAXS pattern at zero protein concentration shown above.

The $I(0)/c$ extrapolated to zero protein concentration $(I(0)/c)_{c\to 0}$ is known to be proportional to a weight-averaged molecular weight (M_w) of solutes as

$$\left(\frac{I(0)}{c}\right)_{c\to 0} = k\frac{\sum_i M_i c_i}{\sum_i c_i} = kM_w, \quad (3)$$

where k is a constant and M_i and c_i are the molecular weight and the weight concentration, respectively, of the ith molecular species (33). The value of k was obtained from the SAXS pattern of the GroEL tetradecamer that has a molecular weight of 8.02×10^5. Equation 3 was applied to the SAXS patterns of GroEL-GroES mixtures, where the GroEL-GroES complexes and free GroEL (or GroES) coexisted (see below).

Theoretical SAXS patterns were obtained by the multipole spherical harmonic expansion method of Svergun et al. (52) using the CRYSOL software package. In all cases, a 3-Å-thick hydration shell with the contrast ($\delta\rho$) of the order 75 e/nm^3 (i.e., 0.075 e/Å^3) and the effective atomic radius (r_0) of 1.8 Å were used in all the scattering calculations. The $P(r)$ profiles were then calculated for the theoretical models using the program GNOM as described above, with the D_{max} chosen based on the longest chord length of the model structure. For the use of the GNOM and CRYSOL software, we consulted the following web site: http://www.embl-hamburg.de/ExternalInfo/Research/Sax/index.html.

RESULTS

Isolated GroEL and GroES characterized by SAXS

Fig. 1 shows the x-ray scattering patterns of isolated GroEL and GroES. We measured the scattering patterns of the protein complexes at different concentrations from 3 to 9 μM for the GroEL tetradecamer and from 10 to 41 μM for the GroES heptamer and extrapolated the patterns to zero protein concentration to reduce the contribution of interparticle interference. The scattering patterns shown in Fig. 1 *a* are those that occur after the extrapolation. We then applied an indirect Fourier transformation method to these scattering patterns using the GNOM software package and obtained the $P(r)$ function for each of the isolated protein oligomers (Fig. 1 *b*) (52). From the $P(r)$, we calculated the radius of gyration, R_g, and the maximum dimension, D_{max}, of the particle (52). The R_g and D_{max} values thus obtained were 67 and 175 Å, respectively, for GroEL and 35 and 100 Å, respectively, for GroES. The R_g values were also obtained from the Guinier plot using Eq. 2, and the values were 69 and 35 Å for GroEL and GroES, respectively (Fig. 1 *c*). The R_g values obtained from the Guinier plot were in good agreement with those from the $P(r)$ analysis, but the value of GroEL from the Guinier plot was ~2 Å larger than that from the $P(r)$. This observation might be due to the presence of small aggregation in free GroEL; the same observation was reported previously by Krueger et al. (53).

For GroEL, we also obtained $P(r)$ profiles and Guinier plots at three different protein concentrations and calculated R_g and D_{max} values from the $P(r)$ as well as R_g and $I(0)/c$ values from the Guinier plot at each protein concentration. Fig. 2 shows the R_g and D_{max} thus obtained from the $P(r)$ and

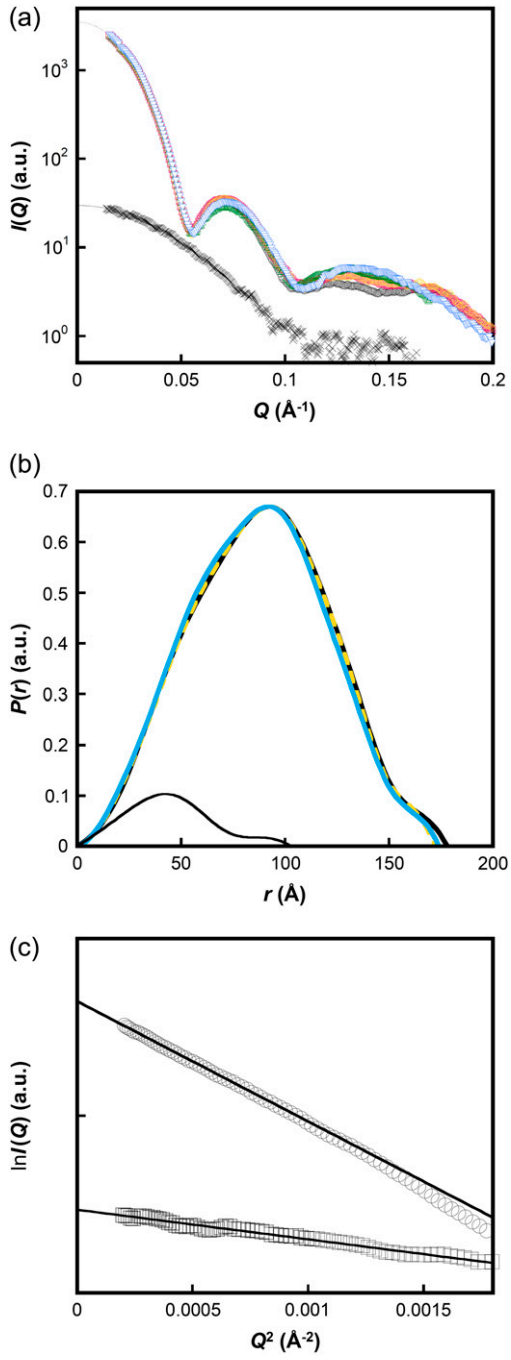

FIGURE 1 (*a*) SAXS patterns of GroEL under various nucleotide conditions and the pattern of GroES (*black crosses*) in the standard buffer (see Materials and Methods) at 25°C. The conditions for GroEL were in the absence of nucleotide (*black circles*) and in the presence of 3 mM ADP (*red squares*), 3 mM ATPγS (*yellow diamonds*), 3 mM ATP (*blue inverted triangles*), and ATP plus BeF_x (*green triangles*). The scattering intensity $I(Q)$ is shown as a function of the momentum transfer Q, which is given by $Q = 4\pi \sin\theta/\lambda$ (λ, wavelength; 2θ, scattering angle). (*b*) The $P(r)$ functions for GroEL in the absence of nucleotide (*thick black line*) and in the presence of ATPγS (*dashed yellow line*) and ATP (*cyan line*) and the $P(r)$ function for GroES (*thin black line*) in the standard buffer. The $P(r)$ functions were calculated using the GNOM software package (51). (*c*) The Guinier plots of GroEL (*open circles*) and GroES (*open squares*). The continuous lines show the least-square fit of the experimental data to Eq. 2 in a Q range of 0.013 Å^{-1} to $1.4/R_g$.

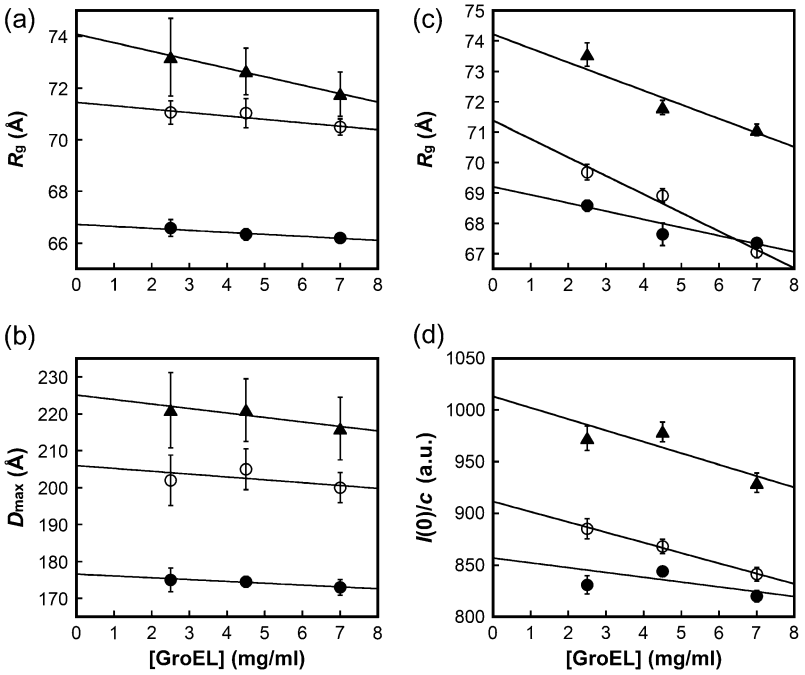

FIGURE 2 R_g (*a*) and D_{max} (*b*) values from the $P(r)$ analysis of isolated GroEL (*solid circles*), the asymmetric GroEL-GroES complex in the presence of 3 mM ATPγS with the [GroES]/[GroEL] ratio (=1) kept constant (*open circles*), and the symmetric GroES-GroEL-GroES complex in the presence of 3 mM ATP plus BeF_x with the [GroES]/[GroEL] ratio (=2) kept constant (*solid triangles*) as a function of GroEL concentration. The R_g (*c*) and $I(0)/c$ (*d*) values from the Guinier plots of isolated GroEL (*solid circles*), the asymmetric GroEL-GroES complex (*open circles*), and the symmetric GroES-GroEL-GroES complex (*solid triangles*) as a function of GroEL concentration. Error bars indicate standard errors of the average estimated from several independent determinations.

the R_g and $I(0)/c$ from the Guinier plot as a function of the GroEL concentration. The extrapolation of the R_g and D_{max} values from the $P(r)$ to zero GroEL concentration gave the values of 67 and 176 Å, respectively, which were essentially identical to the values obtained from the $P(r)$ profiles extrapolated to zero GroEL concentration shown above. The R_g from the Guinier plot (Fig. 2 *c*) shows steeper dependence on the protein concentration than the R_g from the $P(r)$ (Fig. 2 *a*), reflecting the fact that the scattering in the low-Q region used in the Guinier plot is more strongly affected by interparticle interference. Nevertheless, the R_g value from the Guinier plot was 69 Å when extrapolated to zero GroEL concentration, and hence it was identical to the value obtained from the Guinier plot extrapolated to zero GroEL concentration shown above.

The scattering patterns of GroEL in the presence of ATP, ADP, and a nonhydrolyzable ATP analog (ATPγS) are also shown in Fig. 1 *a*. The scattering pattern at 3 mM ATP was also measured in the presence of BeF_x (10 mM NaF plus 300 μM $BeCl_2$) because the presence of both ATP and BeF_x led to the symmetric (football-type) GroES-GroEL-GroES complex when excess GroES was present simultaneously (see below). Although distinct differences in the scattering patterns under different nucleotide conditions were observed in a region of Q larger than 0.1 $Å^{-1}$ in the semilogarithmic plot of log $I(Q)$ versus Q, the corresponding differences in the $P(r)$ profiles were rather minor (Fig. 1 *b*). This is because the $P(r)$ profile reflects the overall shape of GroEL and is affected more strongly by the scattering in the smaller Q region. The presence of ATP shifted the $P(r)$ profile of GroEL to a slightly smaller r by 0.7 Å with a shoulder around 60 Å, and this led to a reduction of the R_g by 0.6 Å. It is known that only ATP induces a cooperative allosteric transition of GroEL (45,54). The presence or absence of BeF_x did not significantly affect the scattering pattern of GroEL at 3 mM ATP.

The changes in the scattering pattern of GroEL induced by the nucleotides were much smaller than the changes in the scattering pattern caused by the GroEL-GroES complex formation (see below), and hence the above changes did not interfere with the following SAXS analysis of the GroEL-GroES complexes.

Because GroEL may coexist with nonnative substrate proteins in vivo, we also investigated the effect of the denatured protein, which binds to GroEL, on the scattering patterns of GroEL. We used disulfide-reduced α-lactalbumin as the denatured substrate protein (35–37) and measured the scattering patterns under the same nucleotide conditions as used above, but in the presence of disulfide-reduced α-lactalbumin in a molar concentration twice as high as those for GroEL, 1 mM DTT, and 1 mM EGTA; DTT and EGTA were required to keep the disulfide bonds of the substrate protein fully reduced. There were only small changes in the scattering patterns with a small increase in the $I(0)$ by a small percentage caused by the presence of the substrate (data not shown), reflecting the binding of the substrate to GroEL. Because the changes in the scattering patterns were much smaller than the changes caused by the GroEL-GroES complex formation, the former changes did not interfere with the following SAXS analysis.

Complex formation of GroEL and GroES

To investigate how many GroES oligomers can simultaneously bind to one GroEL oligomer under physiological conditions, we measured the scattering patterns of mixtures

of GroEL and GroES at different molar ratios under various nucleotide conditions at 10°C, 25°C, and 37°C. Here, we show only the data at 25°C, because we observed no significant differences in the scattering pattern between 10°C and 25°C or between 25°C and 37°C. For each particular molar concentration ratio [GroES]/[GroEL], we measured the scattering patterns at three different GroEL concentrations from 3 to 9 μM with the [GroES]/[GroEL] ratio kept constant. We then obtained the $P(r)$ profiles from these scattering patterns using the GNOM as well as the Guinier plots from the innermost portions of the scattering patterns, from which we calculated the structural parameters, R_g and D_{max} from the $P(r)$ and R_g and $I(0)/c$ from the Guinier plot at each GroEL concentration. These SAXS parameter values were averaged and extrapolated to zero protein concentration (see Fig. 2). We then investigated the dependence of the SAXS parameters thus obtained on the [GroES]/[GroEL] ratio under different nucleotide conditions in the absence and in the presence of denatured α-lactalbumin.

Because in the presence of a nucleotide (ADP, ATP, or ATPγS) the binding constant between free GroEL and GroES is larger than 10^7 M^{-1}, i.e., more than 10 times larger than $1/c$ (27,30,55), essentially all GroES molecules were bound to GroEL under the conditions here when the [GroES]/[GroEL] ratio was less than the stoichiometric number of the GroEL-GroES complex formation. However, in the absence of the nucleotide, we observed no significant binding between GroEL and GroES (see below).

Radius of gyration and maximum dimension

Fig. 3, *a* and *b*, shows the R_g and D_{max} values from the $P(r)$ of the GroEL-GroES mixture as a function of the [GroES]/[GroEL] ratio at 25°C in the absence of the denatured protein. In the absence of the nucleotides, even when we added an increasing amount of GroES to the GroEL solution, the R_g and D_{max} values remained approximately constant, 66.3 and 174 Å for R_g and D_{max}, respectively (Fig. 3). GroEL thus remained in the uncomplexed state under this condition. In contrast, in the presence of ADP, ATP, or ATPγS, the R_g and D_{max} values increased up to ~71.3 and 205 Å, respectively, with increasing GroES concentration. These values were saturated at a [GroES]/[GroEL] ratio of 1, and the further addition of GroES did not increase the R_g and D_{max} values. When both ATP (3 mM) and BeF_x (10 mM NaF and 300 μM $BeCl_2$) were present in the GroEL-GroES mixture, however, the R_g and D_{max} values further increased up to 74.1 and 226 Å, respectively, with a further increase in the GroES concentration; and these values were saturated at a [GroES]/[GroEL] ratio of 2 (Fig. 3, *a* and *b*). These results, therefore, lead to the following conclusions: i), GroES does not bind to GroEL in the absence of the nucleotides; ii), one GroES heptamer binds to one GroEL tetradecamer to form the asymmetric (bullet-type) complex in the presence of ADP, ATP, or ATPγS; and iii), two GroES heptamers simultaneously bind to one GroEL tetradecamer to form the symmetric (football-type) complex in the presence of both ATP and BeF_x.

Fig. 3 *c* shows the R_g values from the Guinier plot of the GroEL-GroES mixture as a function of the [GroES]/[GroEL] ratio at 25°C in the absence of the denatured protein. Although the R_g values for free GroEL were ~2 Å larger than the values obtained from the $P(r)$ analysis, the results of the [GroES]/[GroEL] dependence of R_g were essentially the same as those obtained from the $P(r)$ analysis shown above. In the presence of ADP, ATP, or ATPγS, the R_g thus in-

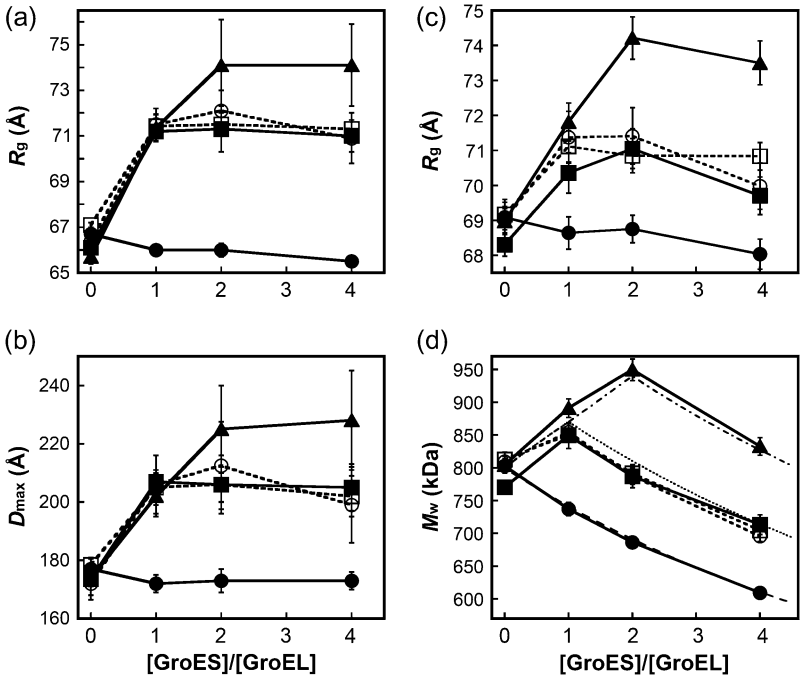

FIGURE 3 Influence of the GroES to GroEL molar concentration ratio, [GroES]/[GroEL], on the complex formation as shown by the radius of gyration (R_g) (*a*) and the maximum distance (D_{max}) (*b*) from the $P(r)$ analysis and by the radius of gyration (R_g) (*c*) and the weight-average molecular weight (M_w) (*d*) from the Guinier plot as a function of [GroES]/[GroEL]. The data were obtained in the absence of nucleotide (*solid circles*) and in the presence of 3 mM ADP (*open squares*), 3 mM ATPγS (*open circles*), 3 mM ATP (*solid squares*), and 3 mM ATP plus BeF_x (*solid triangles*). The GroEL concentration was kept constant at 2.5, 4.5, and 7 mg/ml (3.1, 5.6, and 8.8 μM, respectively). The R_g and D_{max} values from the $P(r)$ analysis were obtained from the scattering pattern at each protein concentration using the GNOM software, and these values were averaged and extrapolated to zero protein concentration (see text). The R_g and M_w values from the Guinier plot were obtained from the slope and the intercept ($I(0)$) of the Guinier plot at each protein concentration, and the values were averaged and extrapolated to zero protein concentration (see text). A thin dotted line and a dot-dash line are the theoretical curves with the stoichiometries of $n_{max} = 1$ and $n_{max} = 2$, respectively, drawn by Eqs. 4–6.

creased up to 71 Å at a [GroES]/[GroEL] ratio of 1, whereas in the presence of both ATP and BeF_x, the R_g further increased up to 74 Å at a [GroES]/[GroEL] ratio of 2.

Although the D_{max} increased with increasing GroES concentration in the same manner as R_g did, the D_{max} may provide additional structural information on the GroEL-GroES complex. The saturated values of D_{max} for the GroEL-GroES mixture when titrated with GroES were 174 Å in the absence of the nucleotides, 205 Å in the presence of ADP, ATP, or ATPγS, and 226 Å in the presence of both ATP and BeF_x. The finding that the D_{max} values were longer in the presence of the nucleotide than in its absence indicates that GroES is located at the longer axis of the GroEL, as shown by crystallographic and electron microscopic studies (7,10–13). The D_{max} values calculated from the x-ray crystallographic structures were 180 and 204 Å for the isolated GroEL tetradecamer (56) and the asymmetric 1:1 GroEL-GroES complex (7), respectively. These values thus coincide well with the observed D_{max} values in the absence of the nucleotides and in the presence of ADP, ATP, or ATPγS, further supporting the above conclusions. The fact that the longest D_{max} value (226 Å) was observed in the presence of both ATP and BeF_x thus demonstrates the formation of the symmetric GroES-GroEL-GroES complex under this condition.

Weight-averaged molecular weight

We also examined the $I(0)/c$ value as a function of the [GroES]/[GroEL] ratio. We calculated the weight-averaged molecular weight M_w from $I(0)/c$ using Eq. 3, and the M_w values thus obtained are plotted as a function of the [GroES]/[GroEL] ratio in Fig. 3 *d*. The M_w value increased with increasing [GroES]/[GroEL] ratio up to 1 in the presence of ADP, ATP, or ATPγS, and up to 2 when both ATP and BeF_x were present in the GroEL-GroES mixture. After reaching the maximum, the observed M_w value decreased with increasing [GroES]/[GroEL] ratio (Fig. 3 *d*).

The dotted line and dot-dash line in Fig. 3 *d* represent theoretical curves of the dependence of M_w on the [GroES]/[GroEL] ratio, under the assumption that GroES is strongly bound to GroEL. The binding between GroEL and GroES is known to be sufficiently strong in the presence of the nucleotide (ADP, ATP, or ATPγS) (27,30,55) (see above), and hence all the GroES molecules must be bound to GroEL when the [GroES]/[GroEL] ratio (γ) is less than the stoichiometric number (n_{max}) of the GroEL-GroES complex. Therefore, when $\gamma \leq 1$, only free GroEL and the asymmetric 1:1 GroEL-GroES complex are present in solution, and hence M_w is given by

$$M_w = \frac{M_{EL}^2(1-\gamma) + (M_{EL} + M_{ES})^2\gamma}{M_{EL} + M_{ES}\gamma}, \quad (4)$$

where M_{EL} and M_{ES} are the molecular weights of the GroEL tetradecamer (8.02×10^5) and the GroES heptamer (7.2×10^4), respectively, and here we also assume the negative cooperativity of the two rings of GroEL with respect to the GroES binding, so that the *trans* ring of the 1:1 GroEL-GroES complex is not occupied by GroES. When $n_{max} = 2$ and $1 < \gamma \leq 2$, only the asymmetric 1:1 and the symmetric 1:2 GroEL-GroES complexes are present, and there is no free GroEL in solution. The M_w is thus given by

$$M_w = \frac{(M_{EL} + M_{ES})^2(2-\gamma) + (M_{EL} + 2M_{ES})^2(\gamma - 1)}{M_{EL} + M_{ES}\gamma}. \quad (5)$$

When γ is larger than the stoichiometric number n_{max} of the complex, the GroES binding to GroEL is saturated, and hence only the saturated GroEL-GroES complex and excess free GroES are present in solution. The M_w is thus given by

$$M_w = \frac{(M_{EL} + n_{max}M_{ES})^2 + M_{ES}^2(\gamma - n_{max})}{M_{EL} + M_{ES}\gamma}. \quad (6)$$

The dotted line in Fig. 3 *d*, a theoretical curve with $n_{max} = 1$ indicating the formation of the asymmetric 1:1 GroEL-GroES complex, shows excellent agreement with experimental data in the presence of ADP, ATP, or ATPγS. The dot-dash line in Fig. 3 *d*, a theoretical curve with $n_{max} = 2$ indicating the formation of the symmetric 1:2 GroEL-GroES complex, shows excellent agreement with the experimental data in the presence of both ATP and BeF_x. Because M_w (or $I(0)/c$) is independent of R_g and D_{max}, these results thus make our conclusions—i), the formation of the asymmetric complex in the presence of ADP, ATP, or ATPγS; and ii), the formation of the symmetric complex in the presence of both ATP and BeF_x—very convincing.

Effect of substrate binding

GroEL in vivo may bind to nonnative substrate proteins, and such binding to the substrate proteins might be an important factor for the complex formation of GroEL and GroES in biological cells (1). To address the question, we repeated the above experiments on the complex formation of GroEL and GroES but in the presence of disulfide-reduced α-lactalbumin, which is known to be denatured and bound to GroEL (35–37); the solution conditions were the same as those used in the experiments in the absence of the denatured protein, except for the presence of 1 mM DTT, 1 mM EGTA, and disulfide-reduced α-lactalbumin at a molar concentration twice as high as the concentration of GroEL. The dependence of the complex formation on the GroES concentration was, however, the same as that in the absence of the denatured protein under each of the nucleotide conditions (data not shown), indicating that the denatured substrate protein has no significant effect on the complex formation of GroEL and GroES. These results strongly suggest that the asymmetric 1:1 GroEL-GroES complex is the major species of the chaperonin within the cell.

Effect of other solution conditions

We further investigated the effect of the simultaneous presence of two different nucleotides (ADP and ATPγS) on the GroEL-GroES complex formation and also the effect of the prolonged incubation with ATP on the complex formation. In the former experiment, we measured the scattering patterns of the GroEL-GroES mixture at three different [GroES]/[GroEL] ratios (i.e., 1, 2, and 3) at 9 μM GroEL in the presence of 0.5 mM ADP and 3 mM ATPγS at 25°C. In the latter experiment, we measured the scattering patterns of the GroEL-GroES mixture (7.5 μM GroEL plus 15 μM GroES) at 3 mM ATP and 25°C at different times (3, 10, 20, 53, 71, and 128 min) after the incubation started. In both the experiments, we observed only the asymmetric 1:1 GroEL-GroES complex. Therefore, neither the presence of the two nucleotides nor the prolonged incubation with ATP was effective for the formation of the symmetric complex.

Structure of the GroEL-GroES complex

To further characterize the structures of the GroEL-GroES complexes, we analyzed the scattering patterns of the asymmetric and the symmetric GroEL-GroES complexes. We used the scattering pattern of the equimolar GroEL-GroES mixture in the presence of ATPγS as the scattering pattern of the asymmetric complex, and the scattering pattern of the mixture at the [GroES]/[GroEL] ratio of 2 in the presence of both ATP and BeF_x as the scattering pattern of the symmetric complex (Fig. 4 *a*). The scattering patterns of the equimolar GroEL-GroES mixture (the asymmetric complex) in the presence of the other nucleotides were the same as that in ATPγS (data not shown). As a control, the scattering pattern of isolated GroEL in 3 mM ATPγS was also investigated (Fig. 4 *a*). All the scattering patterns shown in Fig. 4 have been extrapolated to zero GroEL concentration. Compared with the scattering patterns of isolated GroEL, these scattering patterns show distinct differences in a Q region above 0.07 $Å^{-1}$ in the plot of log $I(Q)$ versus Q. This is in contrast with the previous observation that the nucleotide binding to GroEL led to distinct changes in the scattering pattern only in a region of Q above 0.1 $Å^{-1}$ (Fig. 1 *a*), indicating that the GroES binding to GroEL results in a much larger change in the overall structure of the chaperonin complex than the nucleotide binding to GroEL does. However, it should also be noted that the plots in Fig. 4 are semilogarithmic, and hence changes in $I(Q)$ itself in a smaller Q region (<0.07 $Å^{-1}$), caused by the binding of GroES to GroEL, were not negligible, as clearly indicated by the changes in R_g and D_{max}.

Fig. 4 *b* shows the $P(r)$ functions calculated from these scattering patterns of Fig. 4 *a*. As the number of bound GroES oligomers increased, the peak of the $P(r)$ profile shifted from 93 to 95 Å, and the D_{max} value increased from 174 to 205 Å (see also Fig. 3).

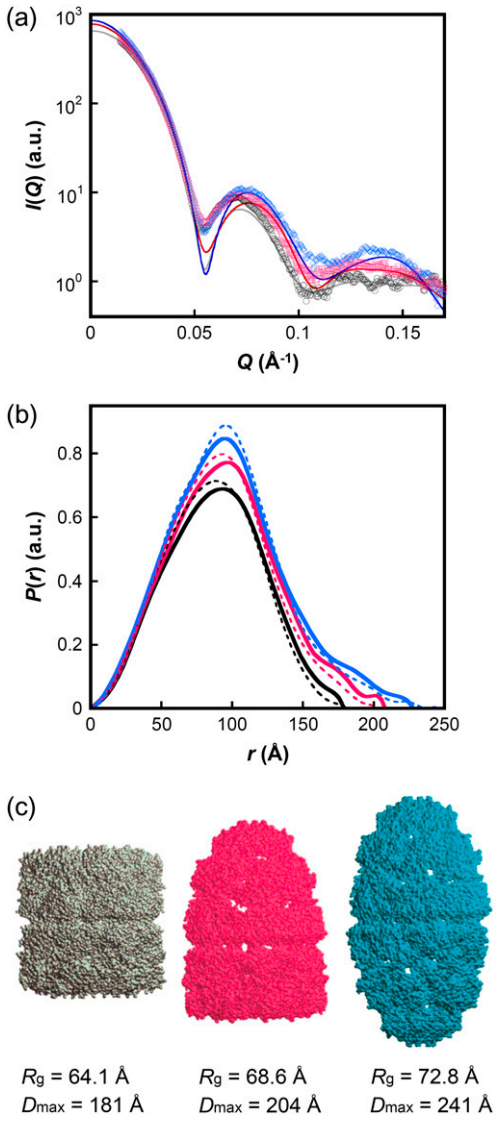

FIGURE 4 SAXS patterns (*a*) and the $P(r)$ functions (*b*) of isolated GroEL (*black circles*), the asymmetric GroEL-GroES complex (*red squares*), and the symmetric GroES-GroEL-GroES complex (*blue diamonds*). The scattering pattern of the mixture of equimolar GroEL and GroES in the presence of ATPγS and that of the mixture containing a twofold molar excess of GroES relative to GroEL in the presence of ATP and BeF_x were used for the asymmetric and the symmetric complexes, respectively. The scattering patterns were measured at different GroEL concentrations from 3 to 9 μM and extrapolated to zero GroEL concentration. The $P(r)$ functions were then calculated from the scattering patterns using the program GNOM. The theoretical scattering curves calculated from the x-ray crystallographic structures of free GroEL oligomer (Protein Data Bank code, 1KP8) (*gray line*) and the asymmetric GroEL-GroES complex (1AON) (*red line*), and the theoretical profile from the putative structure of the symmetric GroES-GroEL-GroES complex (*blue line*) were compared with the experimentally obtained scattering curves (*open symbols*) in (*a*). Similarly, the theoretical $P(r)$ profiles (*dashed lines*) calculated from the x-ray crystallographic structures and the putative complex structure were compared with the experimentally obtained $P(r)$ profiles in *b*. (*c*) The three-dimensional structures of free GroEL (*gray*), the asymmetric GroEL-GroES complex (*magenta*), and the symmetric GroES·GroEL·GroES complex (*cyan*) used for the calculations. The putative structure of the symmetric complex was constructed from the *cis* ring of the asymmetric complex (1AON).

We then calculated the theoretical $P(r)$ profiles of isolated GroEL, the asymmetric complex, and the symmetric complex from the known x-ray structures and compared these theoretical profiles with the experimental ones (Fig. 4 *b*). We employed the x-ray structures of GroEL (1KP8) and the GroEL-GroES-ADP complex (1AON) for isolated GroEL and the asymmetric 1:1 GroEL-GroES complex, respectively (Fig. 4 *c*) (7,56). For the symmetric GroES-GroEL-GroES complex, we constructed a model structure from the *cis* ring of the asymmetric complex (1AON). In this model structure, the two *cis* rings were stacked back-to-back and formed the symmetric GroES-GroEL-GroES complex (Fig. 4 *c*). There are 22 or 23 residues missing at the C-terminus of GroEL in the x-ray coordinates of both 1KP8 and 1AON. Therefore, in all three structures, these unresolved amino acids at the C-terminus of GroEL were modeled using a cylinder that was essentially the same as that employed by Thiyagarajan et al. (57). The cylinder was located at the bottom of each central cavity of GroEL and had a size of 40 Å in diameter and 65 Å in height and a mass of 2.85×10^4.

The theoretical x-ray scattering patterns for the above three structures were calculated using CRYSOL software, and the resultant patterns were transformed into the corresponding $P(r)$ profiles by using GNOM software (51,52). The theoretical scattering patterns and $P(r)$ profiles thus obtained are compared with those observed experimentally in Fig. 4. The theoretical and experimental patterns and profiles are found to be generally in good agreement, although there are some differences observed (see below). The theoretical $P(r)$ profiles reproduced the shifts of the peak and the D_{max} toward larger values with an increasing number of bound GroES oligomers (Fig. 4 *b*). In addition, the theoretical x-ray scattering patterns reproduced the two small peaks at Q values of 0.125 and 0.168 $Å^{-1}$ in isolated GroEL and their collapse into a single peak at a Q of 0.13 $Å^{-1}$ in the asymmetric and symmetric complexes, both of which were observed experimentally (Fig. 4 *a*). Such agreement between the experimental and theoretical $P(r)$ profiles and also between the experimental and theoretical scattering patterns thus indicates that the crystal structures of isolated GroEL (1KP8) and the asymmetric 1:1 GroEL-GroES complex (1AON) well represent their structures in solution and that the putative atomic model of the symmetric GroES-GroEL-GroES complex well represents the conformation of the symmetric complex in solution.

There are, however, small but nontrivial differences between the experimental data and theoretical curves (Fig. 4, *a* and *b*); e.g., a trough observed in the scattering patterns at 0.052 $Å^{-1}$ is significantly deeper in the theoretical curves. These differences may be due to differences between the crystallographic and solution structures of the proteins.

DISCUSSION

Which is predominant under physiological conditions, the asymmetric or the symmetric complex of GroEL and GroES? Although there have been a large number of structural studies of the GroEL-GroES complex, this fundamental question remains to be resolved. Previous structural studies performed by different groups and employing primarily electron microscopy have reported conflicting results. Although the conditions and solutions used were similar, some of the studies reported that only the asymmetric complex was formed (10–13) and others that the symmetric complex was formed as the major species under physiological conditions (15,17,18,20). Whether the asymmetric or the symmetric complex is the major species is indeed of critical importance in considering the molecular mechanisms of the chaperonin cycle. A model in which the symmetric complex appears as an important intermediate in the chaperonin reaction cycle has been proposed by several research groups, including the Fersht group (22), the Buchner group (21,58,59), the Goloubinoff group (24,25), and the Valpuesta group (19), whereas another model in which only the asymmetric complex appears during the reaction cycle has been proposed by the Horwich group (28,30) and the Hartl group (26,27,29).

In addition to the observations of the symmetric 1:2 GroEL-GroES complex by electron microscopy (16–21), chemical cross-linking (15,60), analytical ultracentrifugation (55), and fluorescence techniques (23,61), the most efficient GroEL-mediated refolding reactions of target proteins (Rubisco, mitochondrial malate dehydrogenase, and the Y283D mutant of maltose-binding protein) were known to be attained when the [GroES]/[GroEL] ratio was 2 or greater under a physiological condition in the presence of ATP. This has also been taken as evidence for the requirement of the symmetric football-type 1:2 GroEL-GroES complex as the efficient catalyst of the folding (20,21,60,62).

On the other hand, Hayer-Hartl et al. (29) have shown by the use of rapid cross-linking, native gel electrophoresis, and the refolding assay of malate dehydrogenase that the symmetric complex is not required for chaperonin function, and its presence does not significantly increase the rate of protein folding. Their result thus supports the view that the symmetric 1:2 GroEL-GroES complex has no essential role in the chaperonin mechanism. The acceleration of the refolding rates of the substrate proteins at a molar ratio ([GroES]/[GroEL]) of 2 or greater was previously observed at a nanomolar to submicromolar concentration of GroEL. If we assume that the dissociation constant between the asymmetric complex and GroES was ~ 1 μM, the acceleration was not necessarily caused by the formation of the symmetric 1:2 GroEL-GroES complex (29). Hayer-Hartl et al. have also shown by electron microscopy and rapid cross-linking that the symmetric complex is formed only under an unphysiological condition of a high magnesium concentration (50 mM) and an increased pH (pH 8.0) (26,29).

Rye et al. (28,30) employed stopped-flow fluorescence anisotropy and energy transfer to directly observe the binding and dissociation of GroES and GroEL. They found that the dissociation of the asymmetric GroEL-GroES-ADP

complex was directly and efficiently coupled to the binding of ATP and nonnative substrate protein on the opposite (*trans*) ring; so that this event occurred before another molecule of GroES could bind to the *trans* ring. Their results thus suggest that the symmetric 1:2 GroEL-GroES complex does not accumulate significantly during the chaperonin cycle.

In this study, to resolve the above question about the stoichiometry of the GroEL-GroES complex, we employed the SAXS technique and investigated the structure of the GroEL-GroES complex under various nucleotide conditions. We observed only the asymmetric (bullet-type) complex when excess GroES was present in the presence of ADP, ATPγS, or ATP (3 mM) at pH 7.5 (50 mM Tris-HCl, 10 mM $MgCl_2$, and 100 mM KCl) at 10°C, 25°C, and 37°C; and the presence or absence of the denatured substrate protein (disulfide-reduced α-lactalbumin) did not affect the results. It is thus concluded that the asymmetric complex is the major species under physiological conditions.

Some previous studies have reported that the formation of the symmetric complex depended on the amount of time after the incubation of the GroEL and GroES mixture was started (63) and that the symmetric complex was also formed when ADP and a nonhydrolyzable ATP analog were both present (17,23). Therefore, we also investigated the effect of the prolonged incubation of the GroEL-GroES mixture in 3 mM ATP and the effect of the simultaneous presence of ADP and ATPγS on the GroEL-GroES complex formation. In both cases, however, we observed only the asymmetric GroEL-GroES complex, further strengthening our conclusion that the asymmetric complex is the major species under physiological conditions.

Why did some previous groups observe the symmetric complex under similar conditions? The answer to this question is largely unknown. However, in the electronmicroscopic analysis, which most previous studies used, the side views were subjected to the analysis; and there might be a bias toward the symmetric images, because the symmetric complex always appears in the side view orientation whereas a significant portion of the asymmetric bullet-type complexes may appear in the top view orientation. Chemical cross-linking, which was often used for the stabilization of the complexes in electronmicroscopic studies and electrophoretic analysis (15,18), might also affect the complex formation and stabilize the symmetric GroEL-GroES complex. The SAXS technique has an advantage over the techniques used in the studies that reported the symmetric complex formation. The SAXS pattern directly reflects the structure of the GroEL-GroES complex formed in solution (31–34,53,64); this is in contrast to the techniques such as electron microscopy, chemical cross-linking, and refolding assay, all of which are more or less indirect. Furthermore, the concentration of GroEL ($3 \sim 9$ μM) used in the SAXS experiments here was comparable to the real concentration (2.6 μM) of GroEL in *E. coli* cells (65). Therefore, although some previous studies have reported the formation of the symmetric GroES-GroEL-GroES complex, the observation here by SAXS that only the asymmetric complex was significantly present in solution should leave little doubt that the asymmetric complex is the major species within biological cells.

Although GroEL and GroES formed only the asymmetric complex under physiological conditions, we found that they formed the symmetric (football-type) complex when BeF_x and ATP were both present. In the presence of ATP and BeF_x, the ADP-BeF_x complex was probably bound to the nucleotide-binding site of GroEL, and ATP hydrolysis by GroEL was stalled (42). The symmetric complex may not be perfectly symmetric in terms of the bound nucleotides in the two GroEL rings. One ring may be saturated with ADP-BeF_x, whereas the other ring may be bound to ATP. The analysis of nucleotides extracted from the stable symmetric complex showed, however, that only ADP occupied all 14 nucleotide-binding sites of GroEL, probably due to the hydrolysis of the bound ATP (42). The complex of metal fluoride and ADP strongly stabilizes interactions of the GroEL heptameric (*cis*) ring with GroES (66); and hence the binding of ATP to the *trans* side cannot eject the bound ADP and GroES in the *cis* side, resulting in the formation of the pseudosymmetric GroES-GroEL-GroES complex. It is noted that such a pseudosymmetric complex formed in the presence of ATP and BeF_x was also observed in archaeal group II chaperonin (43).

Because ADP-BeF_x mimics a transient state of ATP hydrolysis (38–41,43), it is suggested that GroEL and GroES may form the symmetric complex transiently during the ATP hydrolysis cycle under physiological conditions. The existence of such a transiently formed symmetric complex is supported by a recent report by Horowitz et al. (67), who have studied the kinetics of binding and dissociation between GroEL and GroES and suggested that the transient formation of the symmetric complex may permit the exchange of a free GroES for the GroES bound in the stable asymmetric complex. The GroES/GroEL molar ratio within *E. coli* cells is known to be 2, indicating that the transient formation of the symmetric complex is feasible in vivo.

We thank Mr. Ryohei Yoshida, Tomotaka Oroguchi, Katsuaki Tomoyori, and Hiroyasu Nakatani for their assistance with the SAXS experiment. We also thank Professor Yasushi Kawata (Tottori University) for providing the expression plasmid (pETESwild) and Professor Yoshiyuki Amemiya and Professor Katsuzo Wakabayashi for giving us the opportunity to use the CCD-based x-ray detector coupled with the beryllium-windowed x-ray image intensifier. The SAXS experiment was performed under the approval of the Photon Factory (proposal Nos. 2000G325, 2002G327, 2004G398, and 2006G384).

This work was supported by Grants-in-Aid for Scientific Research on Priority Areas (project No. 15076201) and for Scientific Research (*B*) (project No. 17370052) from the Ministry of Education, Culture, Science and Technology of Japan.

REFERENCES

1. Fenton, W. A., and A. L. Horwich. 2003. Chaperonin-mediated protein folding: fate of substrate polypeptide. *Q. Rev. Biophys.* 36:229–256.

2. Young, J. C., V. R. Agashe, K. Siegers, and F. U. Hartl. 2004. Pathways of chaperone-mediated protein folding in the cytosol. *Nat. Rev. Mol. Cell Biol.* 5:781–791.
3. Sigler, P. B., Z. H. Xu, H. S. Rye, S. G. Burston, W. A. Fenton, and A. L. Horwich. 1998. Structure and function in GroEL-mediated protein folding. *Annu. Rev. Biochem.* 67:581–608.
4. Thirumalai, D., and G. H. Lorimer. 2001. Chaperonin-mediated protein folding. *Annu. Rev. Biophys. Biomol. Struct.* 30:245–269.
5. Saibil, H. R., and N. A. Ranson. 2002. The chaperonin folding machine. *Trends Biochem. Sci.* 27:627–632.
6. Braig, K., Z. Otwinowski, R. Hegde, D. C. Boisvert, A. Joachimiak, A. L. Horwich, and P. B. Sigler. 1994. The crystal structure of the bacterial chaperonin GroEL at 2.8 Å. *Nature.* 371:578–586.
7. Xu, Z. H., A. L. Horwich, and P. B. Sigler. 1997. The crystal structure of the asymmetric GroEL-GroES-$(ADP)_7$ chaperonin complex. *Nature.* 388:741–750.
8. Weissman, J. S., C. M. Hohl, O. Kovalenko, Y. Kashi, S. Chen, K. Braig, H. R. Saibil, W. A. Fenton, and A. L. Horwich. 1995. Mechanism of GroEL action: productive release of polypeptide from a sequestered position under GroES. *Cell.* 83:577–587.
9. Mayhew, M., A. C. R. Da Silva, J. Martin, H. Erdjument-Bromage, P. Tempst, and F. U. Hartl. 1996. Protein folding in the central cavity of the GroEL-GroES chaperonin complex. *Nature.* 379:420–426.
10. Ishii, N., H. Taguchi, M. Sumi, and M. Yoshida. 1992. Structure of holo-chaperonin studied with electron microscopy: oligomeric cpn10 on top of two layers of cpn60 rings with two stripes each. *FEBS Lett.* 299:169–174.
11. Langer, T., G. Pfeifer, J. Martin, W. Baumeister, and F. U. Hartl. 1992. Chaperonin-mediated protein folding: GroES binds to one end of the GroEL cylinder, which accommodates the protein substrate within its central cavity. *EMBO J.* 11:4757–4765.
12. Saibil, H. R., D. Zheng, A. M. Roseman, A. S. Hunter, G. M. F. Watson, S. Chen, A. Auf der Mauer, B. P. O'Hara, S. P. Wood, N. H. Mann, L. K. Barnett, and R. J. Ellis. 1993. ATP induces large quaternary rearrangements in a cage-like chaperonin structure. *Curr. Biol.* 3:265–273.
13. Chen, S., A. M. Roseman, A. S. Hunter, S. P. Wood, S. G. Burston, N. A. Ranson, A. R. Clarke, and H. R. Saibil. 1994. Location of a folding protein and shape changes in GroEL-GroES complexes imaged by cryo-electron microscopy. *Nature.* 371:261–264.
14. Ranson, N. A., D. K. Clare, G. W. Farr, D. Houldershaw, A. L. Horwich, and H. R. Saibil. 2006. Allosteric signaling of ATP hydrolysis in GroEL-GroES complexes. *Nat. Struct. Mol. Biol.* 13:147–152.
15. Azem, A., M. Kessel, and P. Goloubinoff. 1994. Characterization of a functional $GroEL_{14}$ $(GroES_7)_2$ chaperonin hetero-oligomer. *Science.* 265:653–656.
16. Llorca, O., S. Marco, J. L. Carrascosa, and J. M. Valpuesta. 1994. The formation of symmetrical GroEL-GroES complexes in the presence of ATP. *FEBS Lett.* 345:181–186.
17. Schmidt, M., K. Rutkat, R. Rachel, G. Pfeifer, R. Jaenicke, P. Viitanen, G. Lorimer, and J. Buchner. 1994. Symmetric complexes of GroE chaperonins as part of the functional cycle. *Science.* 265:656–659.
18. Llorca, O., S. Marco, J. L. Carrascosa, and J. M. Valpuesta. 1997. Symmetric GroEL-GroES complexes can contain substrate simultaneously in both GroEL rings. *FEBS Lett.* 405:195–199.
19. Llorca, O., S. Marco, J. L. Carrascosa, and J. M. Valpuesta. 1997. Conformational changes in the GroEL oligomer during the functional cycle. *J. Struct. Biol.* 118:31–42.
20. Sparrer, H., K. Rutkat, and J. Buchner. 1997. Catalysis of protein folding by symmetric chaperone complexes. *Proc. Natl. Acad. Sci. USA.* 94:1096–1100.
21. Beissinger, M., K. Rutkat, and J. Buchner. 1999. Catalysis, commitment and encapsulation during GroE-mediated folding. *J. Mol. Biol.* 289:1075–1092.
22. Corrales, F. J., and A. R. Fersht. 1996. Kinetic significance of $GroEL_{14}\cdot(GroES_7)_2$ complexes in molecular chaperone activity. *Fold. Des.* 1:265–273.
23. Gorovits, B. M., J. Ybarra, J. W. Seale, and P. M. Horowitz. 1997. Conditions for nucleotide-dependent GroES-GroEL interactions. $GroEL_{14}(groES_7)_2$ is favored by an asymmetric distribution of nucleotides. *J. Biol. Chem.* 272:26999–27004.
24. Ben-Zvi, A. P., J. Chatellier, A. R. Fersht, and P. Goloubinoff. 1998. Minimal and optimal mechanisms for GroE-mediated protein folding. *Proc. Natl. Acad. Sci. USA.* 95:15275–15280.
25. Ben-Zvi, A. P., J. Chatellier, A. R. Fersht, and P. Goloubinoff. 1998. Minimal and optimal mechanisms for groE-mediated protein folding. *Proc. Natl. Acad. Sci. USA.* 95:15275–15280. (Erratum in *Proc. Natl. Acad. Sci. USA.* 1999. 96:5890).
26. Engel, A., M. K. Hayer-Hartl, K. N. Goldie, G. Pfeifer, R. Hegerl, S. Mueller, A. C. R. Da Silva, W. Baumeister, and F. U. Hartl. 1995. Functional significance of symmetrical versus asymmetrical GroEL-GroES chaperonin complexes. *Science.* 269:832–836.
27. Hayer-Hartl, M. K., J. Martin, and F. U. Hartl. 1995. Asymmetrical interaction of GroEL and GroES in the ATPase cycle of assisted protein folding. *Science.* 269:836–841.
28. Rye, H. S., S. G. Burston, W. A. Fenton, J. M. Beechem, Z. H. Xu, P. B. Sigler, and A. L. Horwich. 1997. Distinct actions of *cis* and *trans* ATP within the double ring of the chaperonin GroEL. *Nature.* 388: 792–798.
29. Hayer-Hartl, M. K., K. L. Ewalt, and F. U. Hartl. 1999. On the role of symmetrical and asymmetrical chaperonin complexes in assisted protein folding. *Biol. Chem.* 380:531–540.
30. Rye, H. S., A. M. Roseman, S. Chen, K. Furtak, W. A. Fenton, H. R. Saibil, and A. L. Horwich. 1999. GroEL-GroES cycling: ATP and nonnative polypeptide direct alternation of folding-active rings. *Cell.* 97:325–338.
31. Stegmann, R., E. Manakova, M. Roessle, H. Heumann, S. E. Nieba-Axmann, A. Plückthun, T. Hermann, R. P. May, and A. Wiedenmann. 1998. Structural changes of the *Escherichia coli* GroEL-GroES chaperonins upon complex formation in solution: a neutron small angle scattering study. *J. Struct. Biol.* 121:30–40.
32. Roessle, M., E. Manakova, I. Lauer, T. Nawroth, J. Holzinger, T. Narayanan, S. Bernstorff, H. Amenitsch, and H. Heumann. 2000. Time-resolved small angle scattering: kinetic and structural data from proteins in solution. *J. Appl. Cryst.* 33:548–551.
33. Vachette, P., and D. I. Svergun. 2000. Small-angle x-ray scattering by solutions of biological macromolecules. *In* Structure and Dynamics of Biomolecules. E. Fanchon, G. Geissler, J.-L. Hodeau, J.-R. Regnard, and P. A. Timmins, editors. Oxford University Press, New York. 199–237.
34. Doniach, S. 2001. Changes in biomolecular conformation seen by small angle x-ray scattering. *Chem. Rev.* 101:1763–1778.
35. Hayer-Hartl, M. K., J. J. Ewbank, T. E. Creighton, and F. U. Hartl. 1994. Conformational specificity of the chaperonin GroEL for the compact folding intermediates of α-lactalbumin. *EMBO J.* 13:3192–3202.
36. Okazaki, A., T. Ikura, K. Nikaido, and K. Kuwajima. 1994. The chaperonin GroEL does not recognize apo-α-lactalbumin in the molten globule state. *Nat. Struct. Biol.* 1:439–446.
37. Aoki, K., H. Taguchi, Y. Shindo, M. Yoshida, K. Ogasahara, K. Yutani, and N. Tanaka. 1997. Calorimetric observation of a GroEL-protein binding reaction with little contribution of hydrophobic interaction. *J. Biol. Chem.* 272:32158–32162.
38. Combeau, C., and M. F. Carlier. 1988. Probing the mechanism of ATP hydrolysis on F-actin using vanadate and the structural analogs of phosphate BeF_3^- and AlF_4^-. *J. Biol. Chem.* 263:17429–17436.
39. Fisher, A. J., C. A. Smith, J. B. Thoden, R. Smith, K. Sutoh, H. M. Holden, and I. Rayment. 1995. X-ray structures of the myosin motor domain of *Dictyostelium discoideum* complexed with $MgADP\cdot BeF_x$ and $MgADP\cdot AlF_4^-$. *Biochemistry.* 34:8960–8972.
40. Maruta, S., G. D. Henry, T. Ohki, T. Kambara, B. D. Sykes, and M. Ikebe. 1998. Analysis of stress in the active site of myosin accompanied by conformational changes in transient state intermediate complexes using photoaffinity labeling and ^{19}F-NMR spectroscopy. *Eur. J. Biochem.* 252:520–529.

41. Inobe, T., K. Kikushima, T. Makio, M. Arai, and K. Kuwajima. 2003. The allosteric transition of GroEL induced by metal fluoride-ADP complexes. *J. Mol. Biol.* 329:121–134.

42. Taguchi, H., K. Tsukuda, F. Motojima, A. Koike-Takeshita, and M. Yoshida. 2004. BeF_x stops the chaperonin cycle of GroEL-GroES and generates a complex with double folding chambers. *J. Biol. Chem.* 279:45737–45743.

43. Iizuka, R., T. Yoshida, N. Ishii, T. Zako, K. Takahashi, K. Maki, T. Inobe, K. Kuwajima, and M. Yohda. 2005. Characterization of archaeal group II chaperonin-ADP-metal fluoride complexes: implications that group II chaperonins operate as a ''two-stroke engine''. *J. Biol. Chem.* 280:40375–40383.

44. Makio, T., M. Arai, and K. Kuwajima. 1999. Chaperonin-affected refolding of α-lactalbumin: effects of nucleotides and the co-chaperonin GroES. *J. Mol. Biol.* 293:125–137.

45. Inobe, T., T. Makio, E. Takasu-Ishikawa, T. P. Terada, and K. Kuwajima. 2001. Nucleotide binding to the chaperonin GroEL: non-cooperative binding of ATP analogs and ADP, and cooperative effect of ATP. *Biochim. Biophys. Acta.* 1545:160–173.

46. Makio, T., E. Takasu-Ishikawa, and K. Kuwajima. 2001. Nucleotide-induced transition of GroEL from the high-affinity to the low-affinity state for a target protein: effects of ATP and ADP on the GroEL-affected refolding of α-lactalbumin. *J. Mol. Biol.* 312:555–567.

47. Higurashi, T., Y. Hiragi, K. Ichimura, Y. Seki, K. Soda, T. Mizobata, and Y. Kawata. 2003. Structural stability and solution structure of chaperonin GroES heptamer studied by synchrotron small-angle x-ray scattering. *J. Mol. Biol.* 333:605–620.

48. Arai, M., K. Ito, T. Inobe, M. Nakao, K. Maki, K. Kamagata, H. Kihara, Y. Amemiya, and K. Kuwajima. 2002. Fast compaction of α-lactalbumin during folding studied by stopped-flow x-ray scattering. *J. Mol. Biol.* 321:121–132.

49. Amemiya, Y., K. Ito, N. Yagi, Y. Asano, K. Wakabayashi, T. Ueki, and T. Endo. 1995. Large-aperture TV detector with a beryllium-windowed image intensifier for x-ray diffraction. *Rev. Sci. Instrum.* 66:2290–2294.

50. Ito, K., H. Kamikubo, N. Yagi, and Y. Amemiya. 2005. Correction method and software for image distortion and nonuniform response in charge-coupled device-based x-ray detectors utilizing x-ray image intensifier. *Jpn. J. Appl. Phys.* 44:8684–8691.

51. Svergun, D. I. 1992. Determination of the regularization parameter in indirect-transform methods using perceptual criteria. *J. Appl. Cryst.* 25:495–503.

52. Svergun, D., C. Barberato, and M. H. J. Koch. 1995. CRYSOL—a program to evaluate x-ray solution scattering of biological macromolecules from atomic coordinates. *J. Appl. Cryst.* 28:768–773.

53. Krueger, S., S. K. Gregurick, J. Zondlo, and E. Eisenstein. 2003. Interaction of GroEL and GroEL/GroES complexes with a nonnative subtilisin variant: a small-angle neutron scattering study. *J. Struct. Biol.* 141:240–258.

54. Inobe, T., M. Arai, M. Nakao, K. Ito, K. Kamagata, T. Makio, Y. Amemiya, H. Kihara, and K. Kuwajima. 2003. Equilibrium and kinetics of the allosteric transition of GroEL studied by solution x-ray scattering and fluorescence spectroscopy. *J. Mol. Biol.* 327:183–191.

55. Behlke, J., O. Ristau, and H. J. Schoenfeld. 1997. Nucleotide-dependent complex formation between the *Escherichia coli* chaperonins GroEL and GroES studied under equilibrium conditions. *Biochemistry.* 36:5149–5156.

56. Wang, J., and D. C. Boisvert. 2003. Structural basis for GroEL-assisted protein folding from the crystal structure of $(GroEL\text{-}KMgATP)_{14}$ at 2.0 Å resolution. *J. Mol. Biol.* 327:843–855.

57. Thiyagarajan, P., S. J. Henderson, and A. Joachimiak. 1996. Solution structures of GroEL and its complex with rhodanese from small-angle neutron scattering. *Structure.* 4:79–88.

58. Sparrer, H., and J. Buchner. 1997. How GroES regulates binding of nonnative protein to GroEL. *J. Biol. Chem.* 272:14080–14086.

59. Grallert, H., and J. Buchner. 2001. Review: a structural view of the GroE chaperone cycle. *J. Struct. Biol.* 135:95–103.

60. Azem, A., S. Diamant, M. Kessel, C. Weiss, and P. Goloubinoff. 1995. The protein-folding activity of chaperonins correlates with the symmetric $GroEL_{14}(GroES_7)_2$ heterooligomer. *Proc. Natl. Acad. Sci. USA.* 92:12021–12025.

61. Toeroek, Z., L. Vigh, and P. Goloubinoff. 1996. Fluorescence detection of symmetric $GroEL_{14}$ $(GroES_7)_2$ heterooligomers involved in protein release during the chaperonin cycle. *J. Biol. Chem.* 271:16180–16186.

62. Diamant, S., A. Azem, C. Weiss, and P. Goloubinoff. 1995. Increased efficiency of GroE-assisted protein folding by manganese ions. *J. Biol. Chem.* 270:28387–28391.

63. Llorca, O., J. L. Carrascosa, and J. M. Valpuesta. 1996. Biochemical characterization of symmetric GroEL-GroES complexes—evidence for a role in protein folding. *J. Biol. Chem.* 271:68–76.

64. Igarashi, Y., K. Kimura, K. Ichimura, S. Matsuzaki, T. Ikura, K. Kuwajima, and H. Kihara. 1995. Solution x-ray-scattering study on the chaperonin GroEL from Escherichia coli. *Biophys. Chem.* 53:259–266.

65. Lorimer, G. H. 1996. A quantitative assessment of the role of chaperonin proteins in protein folding in vivo. *FASEB J.* 10:5–9.

66. Chaudhry, C., G. W. Farr, M. J. Todd, H. S. Rye, A. T. Brunger, P. D. Adams, A. L. Horwich, and P. B. Sigler. 2003. Role of the γ-phosphate of ATP in triggering protein folding by GroEL-GroES: function, structure and energetics. *EMBO J.* 22:4877–4887.

67. Horowitz, P. M., G. H. Lorimer, and J. Ybarra. 1999. GroES in the asymmetric $GroEL_{14}$-$GroES_7$ complex exchanges via an associative mechanism. *Proc. Natl. Acad. Sci. USA.* 96:2682–2686.